

Effects of chain flexibility on the conformational behavior of a single polymer chain

Zhouting Jiang¹ · Wenhui Dou¹ · Tingting Sun² · Yu Shen³ · Dan Cao¹

Received: 3 June 2015 / Accepted: 4 November 2015 / Published online: 17 November 2015
© Springer Science+Business Media Dordrecht 2015

Abstract Effects of chain flexibility on conformational behavior as a function of temperature have been investigated by coarse-grained molecular dynamics (MD) simulation. The paper presents simulation results regarding the potential energies and structural parameters of a single polymer chain made of 100, 200, or 300 beads with various chain flexibilities. Our simulations exhibit the conformational transition from a random coil to a folded structure demonstrated by the curves of non-bonded potential energy, bond-orientational order parameters and characteristic ratios of real polymer chains with a cooling temperature. In this paper, the comparison between the real polymer chain model involving non-bonded interaction and the ideal polymer chain model in the absence of long-range interaction has also been made. It shows that the main factor inducing structural transition lies in the non-bonded interaction. This result explains clearly that the long-range interaction plays an important role in the polymer folding process. Moreover, the flexibility, as well as the chain length of a real polymer chain, strongly effects on its transition temperature. It also concludes that the changes of bond-torsional potential energy and characteristic ratio with the reduced temperature in the ideal polymer models are independent of chain length, but present different tendencies according to the chain flexibility.

Keywords Chain flexibility · Molecular dynamics simulation · Characteristic ratio

Introduction

Polymers show various structural diversity since they have numerous internal degrees, such as the rotational freedom about three consecutive C-C bonds along a polymer chain. The variation of torsion angles, as the main source of polymer flexibility, give the multitude of conformational arrangements [1]. The chain conformation of a polymer chain, which leads to multiple mechanical and thermodynamical properties, is extensively interesting to industrialists and scientists. The molecular mechanism of crystalline polymers in forming compact folded states has been recently studied [2–6]. Except for the polymer crystallization process, chain flexibility strongly effects the polymer adsorption [7], the interfacial morphology of polymer–silica nanocomposites [8], thermal diffusion, and phase separation phenomenon [9]. Even in the biological field, such as protein folding and DNA self-replication, chain flexibility shows an internal constraint to affect its properties [10, 11]. Therefore, the research on the effect of chain flexibility is not only important under industrial applications but also very meaningful as a scientific issue.

It is well known that different conformations of the polymer molecules may represent their different potential energies according to varying distances and angles between the atoms or groups rotating about the bond. The rotational potential energy in a polymer chain generally exhibits several stable states: *trans* (*t*), *gauche* plus (*g*⁺), and *gauche* minus (*g*[−]) separated by energy barriers. The energy difference between *trans* and *gauche* state $\Delta\varepsilon_{tor}$ determines the relative probability of a torsion angle being in a *gauche* state in thermal equilibrium. The energy barrier ΔE_{tor} between *trans* and

✉ Zhouting Jiang
z.jiang@cjlu.edu.cn

¹ Department of Applied Physics, China Jiliang University, Hangzhou 310018, China

² College of Information and Electronic Engineering, Zhejiang Gongshang University, Hangzhou 310018, China

³ Department of Applied Physics, Zhejiang University of Science and Technology, Hangzhou 310023, China

gauche states determines the dynamics of conformational changes of the polymer chain [1]. Then, the conformational transitions show an important relaxation mode of the motion manifested in numerous physical properties of polymers.

As to the experimental aspect, the structural information on chain flexibility can be obtained from the image of a single molecule chain by atomic force microscopy (AFM) [12], X-ray diffraction [13], and small-angle neutron scattering (SANS) [14, 15]. Some physical models for polymer chains, such as the freely jointed chain (FJC) and the wormlike chain (WLC), have been successfully used to describe flexible, as well as semi-flexible polymer chains [16–18]. Computer simulation is another powerful method to discover the detailed mechanism of molecular structure at an atomistic level. Nowadays, fruitful researches have been carried out in the field of structural formation of macromolecular systems by computer simulation to overcome experimental difficulties [19–21]. Despite the progress of computer power, the simulation for complex materials with all atomic details is still extremely computationally demanding and time consuming. In recent years there has been increasing interest in developing a coarse-gained model of a polymer chain to save the running time [20, 22–25]. Although the simplified representation is not a realistic description of the chemical structure of the macromolecule, it keeps the essential features of the research object, such as the connectivity of the chain molecules, the flexibility and the non-bonded interaction. The present article reports the simulation results achieved by molecular dynamics (MD) method on a single polymer chain, which is simplified as a coarse-gained model with different chain flexibilities, to clarify the physical properties of conformational transition.

Simulation models and methods

To minimize the running time during simulation processes and conclude the general properties of polymers instead of a specific one, the coarse-grained model of a polymer chain is adopted in this article. A single polymer chain is treated as a sequence of beads connected by elastic bonds. The present computational models include real and ideal polymer chains. The real polymer chain model is composed of united beads interacting via the bonded potentials (bond-stretching, bond-bending and bond-torsional potentials) and the non-bonded potentials. The different bond-torsional potential energies are described to identify the effects of chain flexibility on the conformational transition of a single polymer chain. Some of our simulations were performed with the non-bonded interaction switched off to model the ideal polymer chain. The four potential functions of a polymer chain are as follows:

1. The bond-stretching potential energy models the covalent bond connecting adjacent beads as a spring with an

equilibrium value of l_0 rather than as a rigid rod. It takes the form

$$E_{stretch} = \sum_{i=2}^N \frac{1}{2} k_b (l_i - l_0)^2, \quad (1)$$

where l_i is the bond length between beads $i-1$ and i . The equilibrium bond length $l_0 = 0.1530$ nm and the bond-stretching potential energy constant are expressed as $k_b = 2.9288 \times 10^5$ kJ/(nm² mol).

2. The bond-bending potential energy models the harmonic potential to constrain the bond angle at equilibrium angle θ_0 between three successive beads

$$E_{bend} = \sum_{i=3}^N \frac{1}{2} k_\theta (\theta_i - \theta_0)^2, \quad (2)$$

where the equilibrium bond angle $\theta_0 = 1.9107$ rad and θ_i is the bond angle between three beads $i-2$, $i-1$, and i . The bond-bending potential energy constant is $k_\theta = 4.1840 \times 10^2$ kJ/(rad² mol).

3. The bond-torsional potential energy describes the rotation of the three bonds that connect four successive beads along the polymer chain sequence

$$E_{torsion} = \sum_{i=4}^N \frac{1}{2} k_\phi \sum_{n=0}^5 a_n \cos^n \phi_i, \quad (3)$$

where ϕ_i is the dihedral angle of two planes consisting of four consecutive beads $i-3$, $i-2$, $i-1$, and i along the backbone. The constant of torsional energy is expressed as $k_\phi = 8.3680$ kJ/mol. The restriction of torsion angles leads to the chain flexibility in its conformation. Three different bond-torsional potential energies were adopted in our simulation and the parameters a_n ($n=0 \dots 5$) were selected to model the various flexibilities of polymer chains (Table 1).

4. In the real polymer chain models (Model I, II and III), the non-bonded interaction involves the united beads apart by at least three bonds by the truncated 12-6 Lennard-Jones potential

$$E_{LJ} = \sum_{i=1}^N \sum_{j=1}^N 4\varepsilon \left[\left(\frac{\sigma}{r_{ij}} \right)^{12} - \left(\frac{\sigma}{r_{ij}} \right)^6 \right] (j-i \geq 4), \quad (4)$$

where r_{ij} is the distance between beads i and j . The ε sets the strength of the nonlocal interaction. The values of the Lennard-Jones potential parameters are $\varepsilon = 0.8301$ kJ/mol and $\sigma = 0.3624$ nm. In the Models IV, V, and VI, the interactions between beads that are far apart along the chain,

even if they approach each other in space, is not considered, i.e., $\varepsilon=0$ kJ/mol in the ideal polymer chain models.

All the simulation results were presented in terms of reduced units [26]. For example, the reduced temperature $T^*=K_B T/\varepsilon$, the reduced energy $E^*=E/\varepsilon$, and the reduced time $t^*=t\sqrt{\varepsilon/m\sigma^2}$ are used. The list of all parameters used in the present study is given in Table 1. The three different bond-torsional potential energies adopted to define various chain flexibilities in real or ideal polymer models are plotted in Fig. 1. In Fig 1, the highest chain flexibility is achieved in Model III comparing Model I and II because of the minimum value of $\Delta\varepsilon_{tor}$. Then, Model I, II, and III represent the stiff, semi-flexible, and flexible real polymers with the non-bonded interactions among beads. The expressions of bonded potential energies of a single polymer chain are exactly the same in the pairs of Models I–IV, II–V, and III–VI, respectively. The differences between Model pairs I–IV, II–V, and III–VI are those of the non-bonded interactions in latter models that are switched off to represent ideal polymer chains, i.e., $\varepsilon=0$ in Eq. 4. The equilibrium state of a single polymer chain with $N=100, 200, 300$ beads covering a wide temperature range is simulated by the MD method. MD simulations were executed from the random configuration of the single polymer chain exposed to vacuum. The Nose–Hoover method is applied to keep the constant temperature of the system [27, 28].

In the following sections, the detailed results of simulating the real or ideal single polymer chain with various chain flexibilities will be presented. The potential energies, especially bond-torsional and non-bonded energies, as well as structural parameters, such as torsion angle, bond-orientational order, and characteristic ratio have been analyzed in the process of conformational transition by quenching the polymer chain at certain temperatures.

Results and discussion

Bond-torsional potential energy

The temperature dependence of potential energies of a single polymer chain is investigated. As the expressions of bond-stretching/bending potential energies are exactly the same in three real polymer chain models and three ideal polymer chain models from I to VI, bond-torsional and non-bonded potential energies are mainly discussed in this article. The simulation results of reduced bond-torsional potential energy of a single polymer chain versus reduced temperature are shown in Fig. 2. As demonstrated in Fig. 2a, the bond-torsional potential energy increases with increasing temperature in both the cases of the real and ideal polymer chains. Comparing the

simulation results of the real polymer chain in Model I, II, and III, the values of bond-torsional potential energy under certain temperatures are in good agreement with the same chain length of $N=200$ beads. Comparing the results of the ideal polymer chains obtained in Model IV, V, and VI, Fig. 2a also shows that the bond-torsional potential energy of the ideal and flexible polymer chain in Model VI is much higher than that of the ideal polymer chain in the semi-flexible Model V or stiff Model IV under a certain temperature when $T^*\leq 1.0$. With the temperature increasing, the slope of the bond-torsional potential curve in Model VI decreases, and the value of it becomes the minimum among three ideal polymer chain models, when $T^*\geq 1.2$. Consequently, in the case of ideal polymer chain models, the change of bond-torsional energy with temperature is strongly related to the chain flexibility. The lowest growth rate of bond-torsional potential as the function of temperature is observed in Model VI, which represents a more flexible and ideal polymer chain.

The chain length dependence of bond-torsional potential energy is also investigated in our simulation work. According to Eq. 3, the bond-torsional potential energy is the sum of contributions from all torsion angles in a single polymer chain. Then, the bond-torsional potential energy of each torsion angle versus reduced temperature is plotted in Fig. 2b to evaluate the simulation results without the effect of chain length. All bond-torsional potential curves increase with increasing temperature, which show the similar tendency in Fig. 2a. For the ideal polymer chain, the values of bond-torsional potential energy per torsion angle as a function of temperature are independent of chain flexibility and chain length. But in the case of a real polymer chain, the change of bond-torsional potential energy per torsion angle with temperature is related to the chain length, i.e., the increasing tendency of shorter polymers is more obvious than that of longer chains. Comparing the simulation results of real and ideal polymer chains, the slopes of increasing bond-torsional potential energy in the case of ideal polymers are higher than those of real polymer chains. It indicates that the effects of non-bonded interactions involving beads far apart along the polymer chain hinder the increasing tendency of bond-torsional potential energy with the temperature.

Non-bonded potential energy

The non-bonded interactions between beads separated by more than three bonds along the chain backbone are considered to simulate the real polymer chain in Model I, II, and III. In the cases of real polymer chains with the same chain length $N=100$ but different chain flexibilities, the reduced non-bonded potential energies as the function of reduced temperature are shown in Fig. 3a. In this figure, as the reduced temperature keeps increasing, the non-bonded interaction evidently decreases to the minimum value and then increases. Such a

Table 1 Parameters used in the simulation

| | Model I | Model II | Model III | Model IV | Model V | Model VI |
|----------------------------|---|---|---|---|---|---|
| l_0 | 0.1530 nm | 0.1530 nm | 0.1530 nm | 0.1530 nm | 0.1530 nm | 0.1530 nm |
| k_b | 2.9288×10^5 kJ/(nm ² mol) | 2.9288×10^5 kJ/(nm ² mol) | 2.9288×10^5 kJ/(nm ² mol) | 2.9288×10^5 kJ/(nm ² mol) | 2.9288×10^5 kJ/(nm ² mol) | 2.9288×10^5 kJ/(nm ² mol) |
| θ_0 | 1.9107 rad | 1.9107 rad | 1.9107 rad | 1.9107 rad | 1.9107 rad | 1.9107 rad |
| k_θ | 4.1840×10^2 kJ/(rad ² mol) | 4.1840×10^2 kJ/(rad ² mol) | 4.1840×10^2 kJ/(rad ² mol) | 4.1840×10^2 kJ/(rad ² mol) | 4.1840×10^2 kJ/(rad ² mol) | 4.1840×10^2 kJ/(rad ² mol) |
| k_ϕ | 8.3680 kJ/mol | 8.3680 kJ/mol | 8.3680 kJ/mol | 8.3680 kJ/mol | 8.3680 kJ/mol | 8.3680 kJ/mol |
| a_0 | 3.8280 | 3.1715 | 2.1533 | 3.8280 | 3.1715 | 2.1533 |
| a_1 | -1.3100 | -2.2662 | -2.2020 | -1.3100 | -2.2662 | -2.2020 |
| a_2 | 1.4140 | 1.7359 | 1.6540 | 1.4140 | 1.7359 | 1.6540 |
| a_3 | 0.3297 | 1.1502 | 0.4870 | 0.3297 | 1.1502 | 0.4870 |
| a_4 | -2.8280 | -2.7110 | -1.8280 | -2.8280 | -2.7110 | -1.8280 |
| a_5 | 3.3943 | 3.3124 | 3.6943 | 3.3943 | 3.3124 | 3.6943 |
| $\Delta \varepsilon_{tor}$ | 14.6314 kJ/mol | 10.6725 kJ/mol | 6.3927 kJ/mol | 14.6314 kJ/mol | 10.6725 kJ/mol | 6.3927 kJ/mol |
| ΔE_{tor} | 18.8803 kJ/mol | 18.1485 kJ/mol | 14.4046 kJ/mol | 18.8803 kJ/mol | 18.1485 kJ/mol | 14.4046 kJ/mol |
| ε | 0.8301 kJ/mol | 0.8301 kJ/mol | 0.8301 kJ/mol | 0 | 0 | 0 |
| σ | 0.3624 nm | 0.3624 nm | 0.3624 nm | – | – | – |

tendency indicates the structural transition from a random coil to the folded configuration. It is also clearly seen from the snapshots of equilibrium configuration of the real polymer chain with $N=100$ in Model I under various temperatures ($T^*=0.6, 1.1, 1.5$) in Fig. 3a. At low temperatures, the *trans* state is dominated, which makes the folded structure. In the mid-temperatures, a real polymer is partly ordered and the *gauche* states are mainly located in the fold surfaces. At high temperatures, *gauche* states are located everywhere and a real polymer chain takes a random coil. The transition temperature

is also closely related to the chain flexibility, i.e., $T^*=0.8, 1.0$ and 1.1 for real polymer chains in Model III, II, and I, respectively. In other words, the higher the chain flexibility, the lower the transition temperature achieved. In Fig. 3a, the values of non-bonded potential energy with different flexibilities are almost the same when $T^* \geq 1.1$. In the range of low temperature $T^* \leq 1.0$, the lower non-bonded potential energy is achieved in the more flexible polymer chain, i.e., the maximum value of the non-bonded potential energy occurs in the case of a stiff polymer chain in Model I under certain temperature. The major reason is that the real polymer chain with high flexibility can easily overcome the energy barrier to obtain the lower non-bonded potential energy.

In order to reveal the effect of the chain length on the long-range interaction of real polymer chains, the non-bonded potential energy of a single polymer with chain length $N=100, 200$ and 300 beads versus reduced temperature is plotted in Fig. 3b. It shows that the longer polymer chain has the lower non-bonded potential energy because of more bead-pairs, even far away along the polymer sequence, close to each other in space to obtain lower potential energy. Consequently, the numerical range of non-bonded potential energy of long chain $N=300$ beads is from -427.7 to -252.69 , which is the largest scale among the numerical results of three cases of chain length in the same temperature scope $0.5 \leq T^* \leq 1.5$. For the real polymer with chain length $N=300$, the non-bonded potential energy increases slowly with increasing temperature until $T^*=1.1$, which is the opposite tendency a of short chain under the low temperature range, and then increases rapidly as the reduced temperature keeps increasing. The critical temperature of non-bonded potential energy, which is related to the

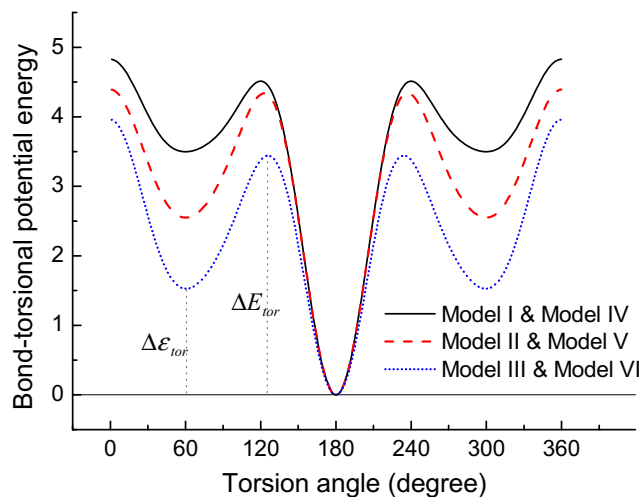


Fig. 1 Reduced bond-torsional potential energy employed to model various chain flexibilities. The *trans* state is the lowest energy conformation located at the torsion angle $\phi=180^\circ$. The two secondary minima corresponding to torsion angle $\phi=60^\circ$ and $\phi=300^\circ$ indicate *gauche* minus and *gauche* plus states. Model I, II, and III represent the stiff, semi-flexible, and flexible polymers, respectively

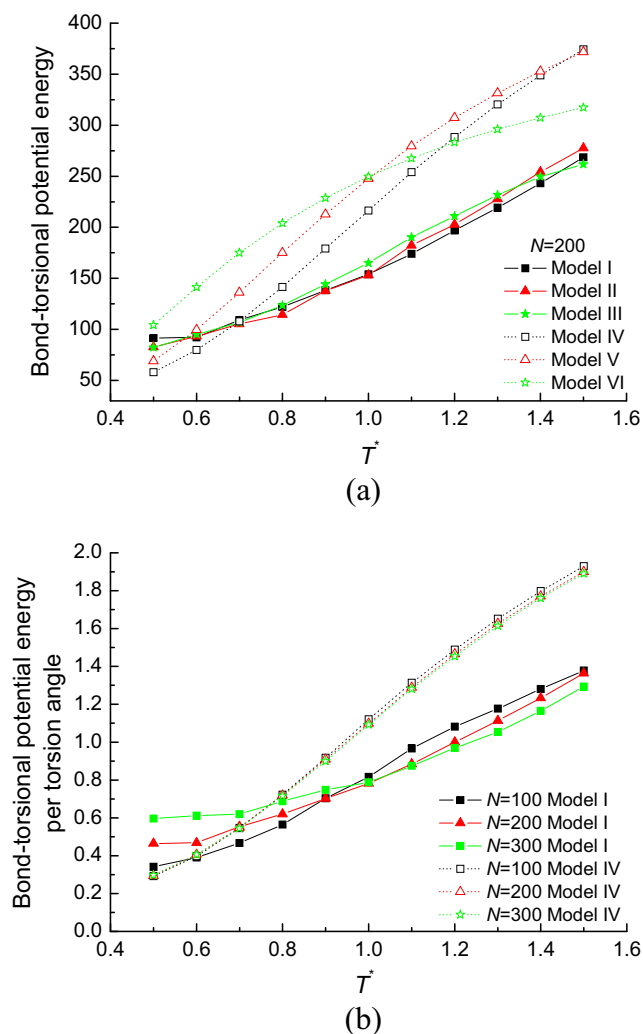


Fig. 2 Reduced bond-torsional potential energy versus reduced temperature T^* . (a): total bond-torsional potential energy of a single polymer chain with chain length $N=200$ beads in six models from I to VI, (b): chain length dependence of bond-torsional potential energy per torsion angle of real polymer (Model I) and ideal polymer (Model IV)

conformational transition, is $T^*=0.8, 0.9$ and 1.1 for the real polymer with chain length $N=100, 2,00$ and 300 beads, respectively. Consequently, for a longer polymer chain, the lower non-bonded potential energy but higher transition temperature is obtained, due to more bead-pairs close in space. These results indicate that the conformational arrangement of a flexible chain can easily adjust to reach a more stable state.

Torsion angle

The probability distribution of torsion angles along a polymer with the same chain length $N=200$ beads at $T^*=0.7$ and 1.3 in six models from I to VI is shown in Fig. 4. It is seen that the conformation of torsion angles predominantly prefers the *trans* state when the chain forms a folded structure at low temperature. With the increasing temperature from 0.7 to

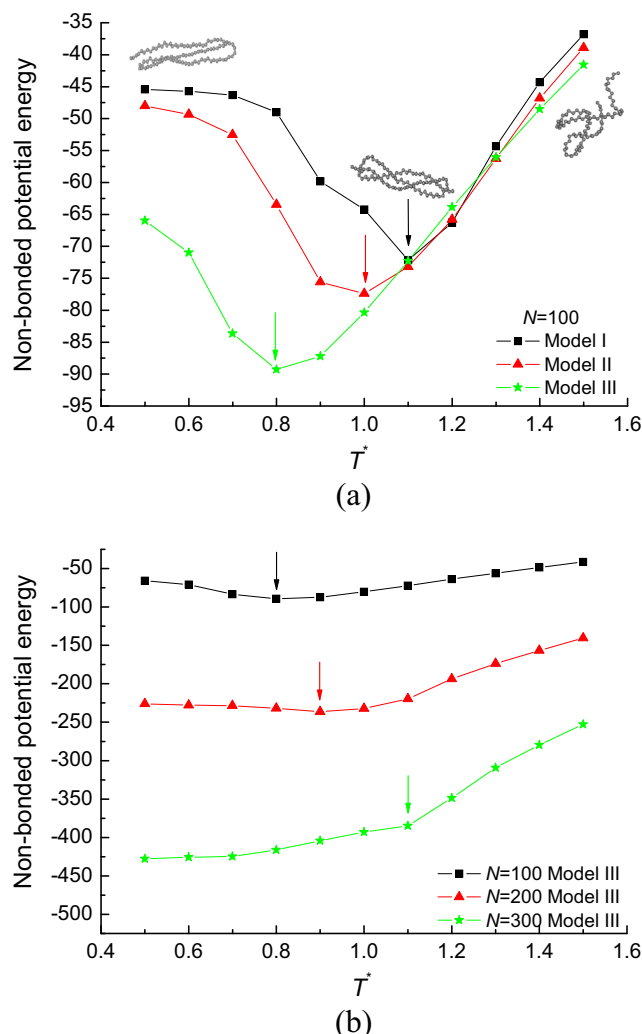


Fig. 3 Reduced non-bonded potential energy versus reduced temperature T^* . (a): non-bonded potential energy of a real polymer chain with various chain flexibilities, (b): chain length dependence of non-bonded potential energy of real polymer chains in Model III

1.3 , the probability of *gauche* state increases. Comparing vertically, such an increasing tendency of the *gauche* state is more obvious for flexible chains in Model III and VI. Comparing the simulation results on real chains (left column) and ideal chains (right column) horizontally in Fig. 4, the probability of a *trans* state of a polymer chain with non-bonded interactions is much higher than that of a polymer chain without non-bonded interactions. When the temperature increases from 0.7 to 1.3 , the increasing probability of a *gauche* state is more evident in the case of ideal chains shown in the right column. Consequently, the increasing tendency of a *gauche* state with the rise of temperature occurs in the cases of more flexible and ideal polymer chains.

As the probability distribution of the torsion angles is completely axis-symmetric along $\phi=180^\circ$, the average value of torsion angles along a polymer chain is analyzed in the range of 0° to 180° . The simulation results of the average

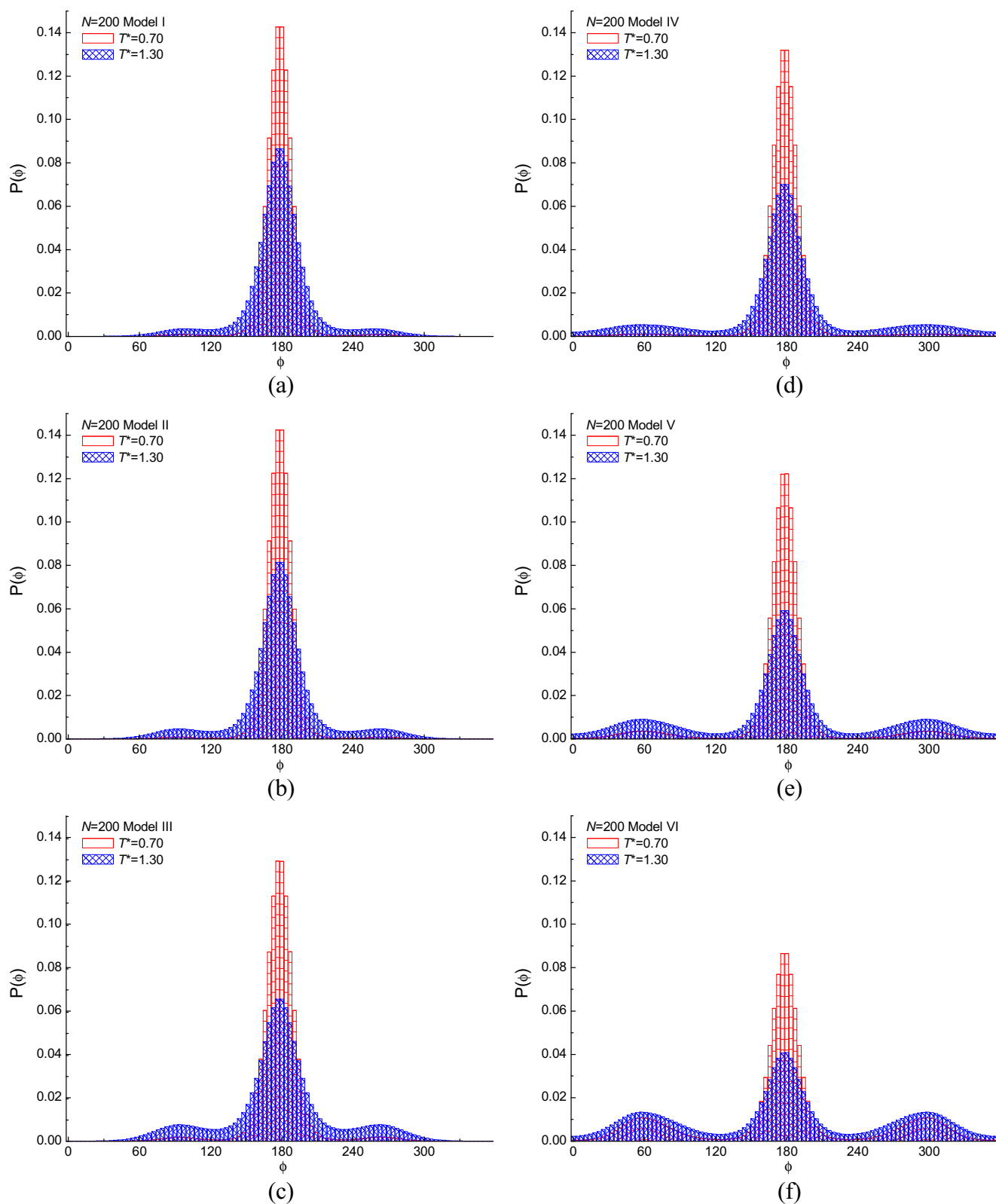


Fig. 4 Probability distribution of torsion angles ϕ with a polymer chain length $N=200$ beads at reduced temperature $T^*=0.7$ and 1.3. (a): the real polymer chain in Model I, (b): the real polymer chain in Model II, (c): the

real polymer chain in Model III, (d): the ideal polymer chain in Model IV, (e): the ideal polymer chain in Model V, and (f): the ideal polymer chain in Model VI

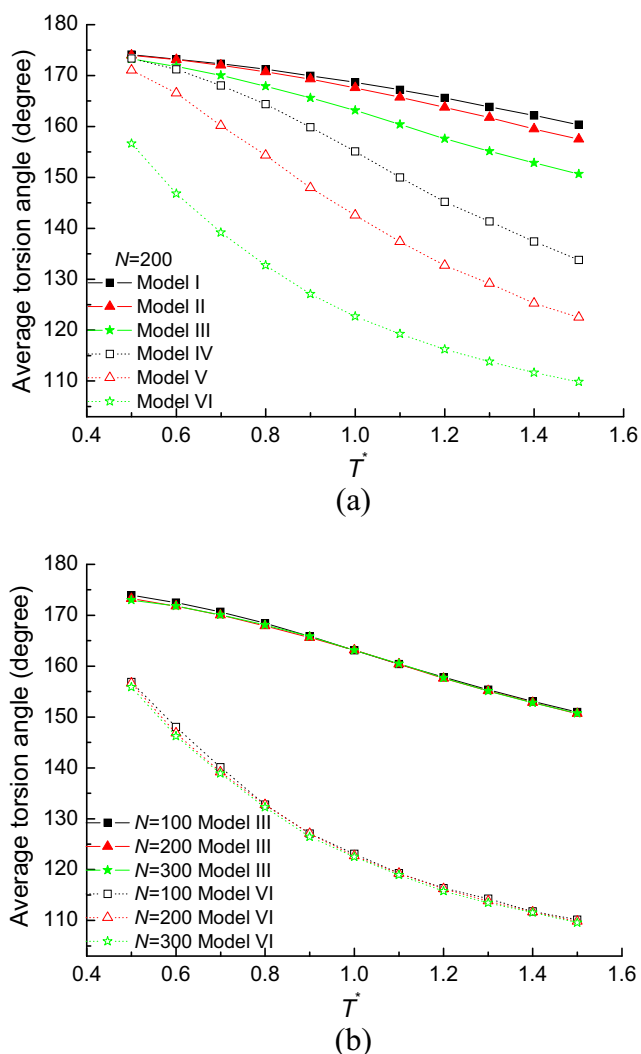


Fig. 5 Average torsion angle versus reduced temperature T^* . (a): average torsion angle of a single polymer chain with chain length $N=200$ beads in six models from I to VI, (b): chain length dependence of average torsion angle of real polymer (Model III) and ideal polymer (Model VI)

torsion angle as the function of temperature is shown in Fig. 5. In Fig. 5a, the average value of the torsion angle decreases with the increasing temperature, and the trend is more significant in the case of the ideal polymer chain with higher flexibility. Under a certain temperature, the smaller average torsion angle of the polymer with higher chain flexibility is obtained, which indicates that the probability distribution of torsion angles in a *trans* state in a flexible chain is lower than the one of a stiff chain. Moreover, the average torsion angle of the ideal polymer is much smaller than that of real ones under certain temperatures, which demonstrates the probability distribution of torsion angles in a *trans* state in an ideal chain is lower than the one of a real polymer chain.

The average torsion angle of a single polymer with chain length $N=100, 200, 300$ beads as the function of reduced temperature is presented in Fig. 5b. As the same tendency in

Fig. 5a, the average torsion angle decreases with increasing temperature. The decreasing tendency of an ideal polymer chain in the Model VI is more obvious than that of a real polymer chain with non-bonded interactions in Model III. As for the same results in Fig. 5a, under a certain temperature, the average torsion angle of the real polymer chain in Model III is larger than the torsion angle of the ideal polymer chain in Model VI. Another interesting result shown in Fig. 5b is that the change of average torsion angle as the function of temperature is independent of chain length whatever is the case of real or ideal polymer chains.

It is well known that the polymer chain has the ability to overcome the energy barrier due to enough kinetic energy at high temperature. Then the high temperature increases the mobility of a polymer chain to achieve a more stable configuration. Except for the effect of the temperature, the results in Figs. 4 and 5 also indicate that the chain flexibility improves the mobility of a polymer chain. But non-bonded interactions involving beads far apart along the polymer chain hinder the adjustment of the chain conformation to reach a more stable state.

Characteristic ratio and bond-orientational order parameter

The characteristic ratio $\langle h^2 \rangle / nl_0^2$ depends on the local flexibility of the polymer chain. The occurrence of *trans-gauche* conformational transitions was monitored by evaluating the characteristic ratio for chain dimensions as a function of temperature, where h is the end-to-end distance of a polymer chain and n is the bond number that is equal to $N-1$. The

bond-orientational order parameter $\sum_{i=3}^N (3\cos^2\phi_i - 1) / 2$ ($N-2$) would be one of the quantitative indicators to describe the structural transitions. Here ϕ_i is the angle between the bond vector and the z-axis of the chain molecule coordinate system. It takes a value of 1 for a polymer chain whose bonds are perfectly parallel, and 0 for randomly orientation. Figure 6a illustrates the variation of the characteristic ratio and bond-orientational order parameter with temperature for chain length $N=200$ beads with different chain flexibilities including or excluding non-bonded potential energy from Model I to Model VI. At high temperatures $T^* > 1.2$, the value of the characteristic ratio for real polymer chains increases slowly as the temperature decreases. It indicates the characteristic features of a random coil, in which *gauche* states are located everywhere. In the medium temperature range $1.0 \leq T^* \leq 1.2$, the value of $\langle h^2 \rangle / nl_0^2$ increases sharply with decreasing temperature leading to a large growth rate of the characteristic ratio. After the characteristic ratio reaching a plateau, it again increases slowly with decreasing temperature, which indicates that the orientationally ordered structure is formed. Then *trans-gauche* conformational change of a real polymer

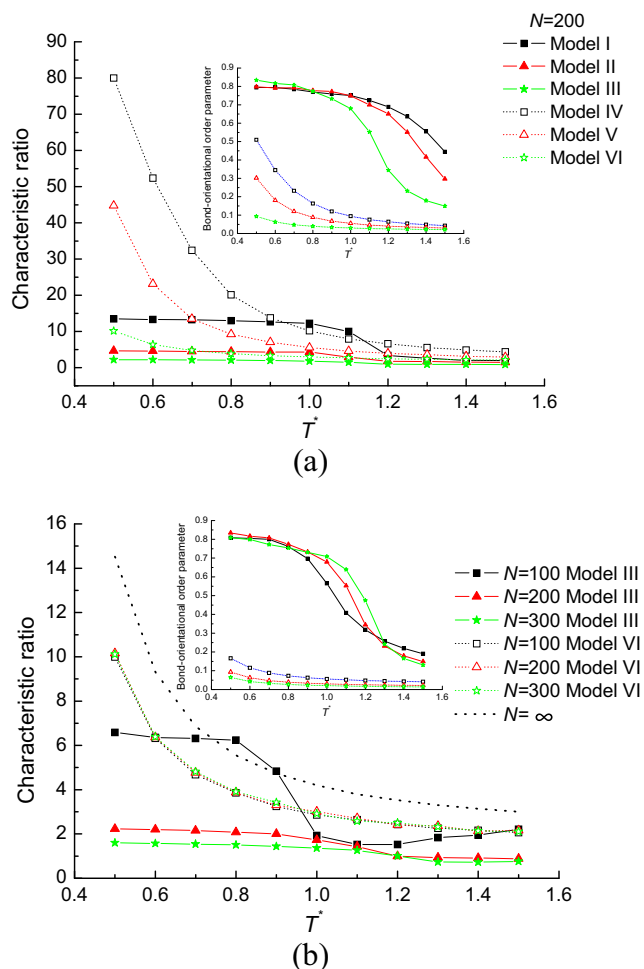


Fig. 6 Characteristic ratio and bond-orientational order parameter versus reduced temperature T^* . (a): characteristic ratio and bond-orientational order parameter (in the inserted figure) of a single polymer chain with chain length $N=200$ beads in six models from I to VI, (b): chain length dependence of characteristic ratio and bond-orientational order parameter (in the inserted figure) of real polymer (Model III) and ideal polymer (Model VI) and comparing with theoretical results in the hindered rotation chain model

chain ceases and only the local motion of united atoms with no global change take place. Such a tendency is more obvious in Model I, which shows the high transition temperature for stiff polymer chains. Comparing the insert figure, the value of bond-orientational order parameter for real polymer chains sharply increases with decreasing temperature till the plateau, which indicates the polymer chain takes anisotropic configuration. Under low temperature, the value of bond-orientational order parameters is close to 1 in the case of a flexible polymer chain in Model III with low transition temperatures. On the contrary, for an ideal polymer chain, the characteristic ratio and the bond-orientational order parameter keep the same tendencies as the function of temperature, i.e., both structural parameters remain increasing with decreasing temperature, and the transition temperatures are not found. The slope of

increasing tendency is especially large for the stiff chains at low temperatures.

The characteristic ratio and the bond-orientational order parameter of a single polymer with chain length $N=100, 2,00$ and 300 beads as the function of reduced temperature are also shown in Fig. 6b. The changes of the characteristic ratio of ideal polymer chains are independent of chain length. The value of the characteristic ratio is increasing with the decreasing temperature, which presents the same tendency as the theoretical value predicated in the hindered rotation chain model. But under certain temperatures, the theoretical characteristic ratio in the hindered rotation chain model is higher than the simulation result in the ideal polymer chain obtained by the MD method. The reason lies in the negligence of the variation of bond angle with temperature in the hindered rotation model. The conformational transitions are also shown in Fig. 6b in the case of real polymer chains. By cooling the temperature, the values of the characteristic ratio is increased rapidly in the mid-temperature scope, especially for a short polymer chain. The transition temperature from the random coil to the ordered structure of the short chain is lower than the for the long polymer chain. Comparing the curves of non-bonded potential energy as the function of temperature in Fig. 3b, the transition temperatures of the characteristic ratio in real polymer models are the same as the ones for non-bonded potential energy, i.e., $T^*=0.8, 0.9$ and 1.1 for chain length $N=100, 2,00$ and 300 beads, respectively. In the insert figure of Fig. 6b, the change of curves for real polymer chains present the random coil to ordered structure transition has occurred. The critical temperature related to the structural factor is chain length dependent, i.e., the transition temperature decreases with short polymer chains. These results suggest that the long range interactions play the key effect on the conformational transition.

Conclusions

In this article, we have carried out MD simulations on the real and ideal polymer chains with various chain lengths and flexibilities under a wide temperature range $0.5 \leq T^* \leq 1.5$. The bond-torsional and non-bonded potential energies of a single polymer chain, as well as structural parameters such as torsion angle, characteristic ratio, and bond-orientational order parameter were discussed in detail. The current numerical results indicate:

- (I) The value of bond-torsional potential energy increases with increasing temperature. The curves of bond-torsional potential energy of real polymer chains with different chain flexibilities are almost overlapping. On the contrary, the bond-torsional potential energy of ideal polymer chains with the same chain length is strongly related to the chain flexibility. With certain chain

flexibility, the bond-torsional potential energy of each torsion angle of the ideal polymer chain is independent of chain length. But in the case of real polymer chains, the slope of increasing bond-torsional potential energy of each torsion angle with increasing temperature for a long chain is lower than that of a short chain.

- (II) The non-bonded potential energy as the function of temperature is investigated in the real polymer models with various chain flexibilities. The simulation results show that with the decreasing temperature, the non-bonded potential energy of real polymer chains decreases to the minimum value and then increases. It also presents the structural transition from a random coil to the folded state by snapshots of the equilibrium configuration of the real polymer chain. The more flexible a chain is, the lower minimum of non-bonded potential energy obtains, which leads to the lower transition temperature. The non-bonded potential energy of the real polymer chain with a certain length is independent of chain flexibility when the temperature is higher than its transition temperature. But the non-bonded potential energy of a longer polymer chain is lower than that of a short polymer. Because of many closed bead-pairs in space, the lower non-bonded potential energy of a longer polymer chain is obtained.
- (III) The conformation of torsion angles predominantly prefers the *trans* state at low temperature. With increasing temperature, the probability of a *gauche* state increases, especially in the case of the ideal polymer chain with high flexibility. The average value of torsion angles decreases with increasing temperature, which is independent of chain length and rather obvious for the flexible polymer chain even without non-bonded interactions among beads.
- (IV) The characteristic ratio, as well as the bond-orientational order parameter of a real polymer chain, shows the clear transition from the random coil to the ordered structure. But in the ideal chain models, the value of the characteristic ratio keeps increasing with the decreasing temperature, as is the same tendency for the bond-orientational order parameter as a function of temperature. Such increasing tendency with cooling temperature is more subtle in the case of a flexible chain, and it is independent of chain length. Comparing the theoretical value of the characteristic ratio predicated in the hindered rotation chain model, the simulation result is lower than the theoretical one under a certain temperature because of ignoring the variation of bond angle with temperature in the hindered rotation model.

Finally, these simulation results of the conformational behavior of a single polymer chain indicate the folded structure is mainly induced by non-bonded interactions involved between beads far apart along the polymer chain but close each other in

space. The higher flexibility of polymer chain leads to more segments in the *gauche* state. Consequently, in the case of the flexible polymer chain, it is hard to form rigid stems, and the conformational transition from random coil to the orientated structure is weakened. Therefore, our study may be profitably used as a guide towards understanding the structural transition of polymer chains and establishing the type of a typical one.

Acknowledgments The authors acknowledge the financial support of the National Natural Science Foundation of China (Grant No. 21204078, 11304282 and 51402275) and the Natural Science Foundation of Zhejiang Province (Grant No. LY12B04003). The computations for this research were performed using the Shuguang HPC supercomputer of China Jiliang University.

References

- Rubinstern M, Colby H (2004) Polymer physics. Oxford University, New York
- Kimata S, Sakurai T, Nozue Y, Kasahara T, Yamaguchi N, Karino T, Shibayama M, Kornfeld JA (2007) Science 316(5827):1014–1017
- Li L, Li CY, Ni C (2006) J Am Chem Soc 128(5):1692–1699
- Loo YL, Register RA, Ryan AJ, Dee GT (2001) Macromolecules 34(26):8968–8977
- Reiter G, Castelein G, Sommer JU, Rottele A, Thurn-Albrecht T (2001) Phys Rev Lett 87(22):226101–226101
- Strobl G (2006) Prog Polym Sci 31(4):398–442
- Linse P, Kallrot N (2010) Macromolecules 43(4):2054–2068
- Zhu A, Cai A, Zhou W, Shi Z (2008) Appl Surf Sci 254(13):3745–3752
- Stadelmaier D, Koehler W (2009) Macromolecules 42(22):9147–9152
- Gruebele M (1999) Annu Rev Phys Chem 50:485–516
- Kuznetsov SV, Shen YQ, Benight AS, Ansari A (2001) Biophys J 81(5):2864–2875
- van Noort J, van der Heijden T, de Jager M, Wyman C, Kanaar R, Dekker C (2003) Proc Natl Acad Sci U S A 100(13):7581–7586
- Nishida K, Okada K, Asakawa H, Matsuba G, Ito K, Kanaya T, Kaji K (2012) Polym J 44(1):95–101
- Gabel F, Lensink MF, Clantin B, Jacob-Dubuisson F, Villeret V, Ebel C (2014) Biophys J 107(1):185–196
- Le RK, Harris BJ, Iwuchukwu IJ, Bruce BD, Cheng X, Qian S, Heller WT, O'Neill H, Frymier PD (2014) Arch Biochem Biophys 550:50–57
- Karayianis NC, Foteinopoulou K, Laso M (2009) J Chem Phys 130(16):164908
- Lei J (2010) J Chem Phys 133(10):104903
- Mansfield ML, Douglas JF (2008) Macromolecules 41(14):5412–5421
- Chen J, Mao J, Thakur S, Xu J, Liu F (2011) J Chem Phys 135(9):094504
- Li T, Jiang Z, Yan D, Nies E (2010) Polymer 51(23):5612–5622
- Sakae Y, Okamoto Y (2010) Mol Simul 36(2):138–158
- Jiang Z, Zhang L, Chen J, Xia A, Zhao D (2002) Polymer 43(22):6037–6047
- Jiang Z, Zhang L, Chen J, Zhao D (2002) Polymer 43(4):1461–1466
- Marrink SJ, de Vries AH, Mark AE (2004) J Phys Chem B 108(2):750–760
- Rossi G, Monticelli L (2014) J Phys Condens Matter 26(50):503101
- Jiang Z, Xu P, Sun T (2012) Chin J Polym Sci 30(1):45–55
- Hoover WG (1985) Phys Rev A 31(3):1695–1697
- Nose S (1984) J Chem Phys 81(1):511–519